



HAL
open science

4H-SiC PiN diode protected by narrow field rings investigated by the micro-OBIC method

Dominique Planson, C Sonnevile, Pascal Bevilacqua, L V Phung, B Asllani,
D Tournier, P Brosselard

► **To cite this version:**

Dominique Planson, C Sonnevile, Pascal Bevilacqua, L V Phung, B Asllani, et al.. 4H-SiC PiN diode protected by narrow field rings investigated by the micro-OBIC method. ECSCRM 2020-2021, Oct 2021, Tours, France. hal-03410274

HAL Id: hal-03410274

<https://hal.science/hal-03410274>

Submitted on 4 Nov 2021

HAL is a multi-disciplinary open access archive for the deposit and dissemination of scientific research documents, whether they are published or not. The documents may come from teaching and research institutions in France or abroad, or from public or private research centers.

L'archive ouverte pluridisciplinaire **HAL**, est destinée au dépôt et à la diffusion de documents scientifiques de niveau recherche, publiés ou non, émanant des établissements d'enseignement et de recherche français ou étrangers, des laboratoires publics ou privés.

4H-SiC PiN diode protected by narrow field rings investigated by the micro-OBIC method

D. Planson^{1, a, *}, C. Sonnevile^{1, b}, P. Bevilacqua^{1, c}, L V Phung^{1, d}, B Asllani^{1, e},
D. Tournier^{2, f}, P. Brosselard^{2, g}

¹Univ Lyon, INSA Lyon, Université Claude Bernard Lyon 1, Ecole Centrale de Lyon, CNRS, AMPERE, F-69621, Lyon, France

²Caly Technologies, 62 Boulevard Niels Bohr, CS52132, F-69603 Villeurbanne Cedex, France

dominique.planson@insa-lyon.fr, camille.sonneville@insa-lyon.fr,
pascal.bevilacqua@insa-lyon.fr, luong-viet.phung@insa-lyon.fr, besar.asllani@insa-lyon.fr,
d.tournier@caly-technologies.com, p.brosselard@caly-technologies.com,

* corresponding author

Keywords: 4H-SiC bipolar diode, high voltage device, electro-physical characterisation, periphery protection, OBIC.

Abstract. This paper presents micro-OBIC measurements performed at different voltages on two devices protected by narrow field rings. At the surface of the device #1, a polyimide layer was deposited during the fabrication process. On the contrary, passivation layer was removed on device #2. Thanks to the micro-OBIC micrometer spatial resolution and the spot size was carefully focused, small gaps in the range of 1 μm can be visible on OBIC profiles. Thus, the variation of the $\mu\text{-obic}$ accurately reflects the topology of each ring.

Introduction

Silicon Carbide (SiC) is an attractive semiconductor material for high power and high temperature applications. To reach the expected breakdown voltage, an effective junction termination is required to spread the electrical field profile towards edges mitigating the crowding effect. Among different techniques used for periphery protection [1], Junction Termination Extension (JTE) is a well-known technique often chosen due to their relative design simplicity. However, the structure of the present paper rely exclusively on guard rings, a more challenging approach where small technological deviations on the rings position can completely negate the benefits of the periphery protection. To get the most from those rings, key parameters such as the distance between each ring and the number of rings must be carefully chosen. The efficiency of this periphery protection is optimal when the electric field at the edge of each ring is nearly equal for all rings. Optical Beam Induced Current (OBIC) technique is a non-destructive powerful technique to analyze the electric field distribution at the edge of the device periphery. This technique has been used to investigate silicon diodes protected by field rings [2], with spacing greater than 10 μm , as well as 4H-SiC PiN diodes protected by JTE [3], [4]. In this paper, micro-OBIC technique is applied to SiC high voltage bipolar diodes where the design of the guard rings is more tightly constrained to analyze the experimental behavior of the periphery protection with respect to the applied reverse voltage.

Experimental Setup

In the micro-OBIC experimental setup, a 349 nm UV pulsed laser is used to generate electron-hole pairs (EHPs). A set of properly adjusted optics (mirrors, microscope objective ...) is inserted on the beam path to finally get a focused laser spot with a diameter of about 1-4 μm as shown on Fig. 1. The sample is placed on a motorized stage and the position is controlled with LabView (i.e. on X, Y, Z automatically and teta manually) of the focal point. The energy at the top surface of the device is high enough to generate electron-hole pairs (EHPs), so that an OBIC current could be measured. The micro-OBIC principle has already been described in [4].

The testbench allows us to realize a spatial mapping of OBIC signal, either on a (X, Y) plane or only on X (or Y) lines. For X or Y lines, the step between two displacements of the laser beam is 200 nm, Anode-Cathode biased. The DUT can be reverse biased by applying voltage up to 500V thanks to the SMU (Source Measure Unit) Keithley 237.

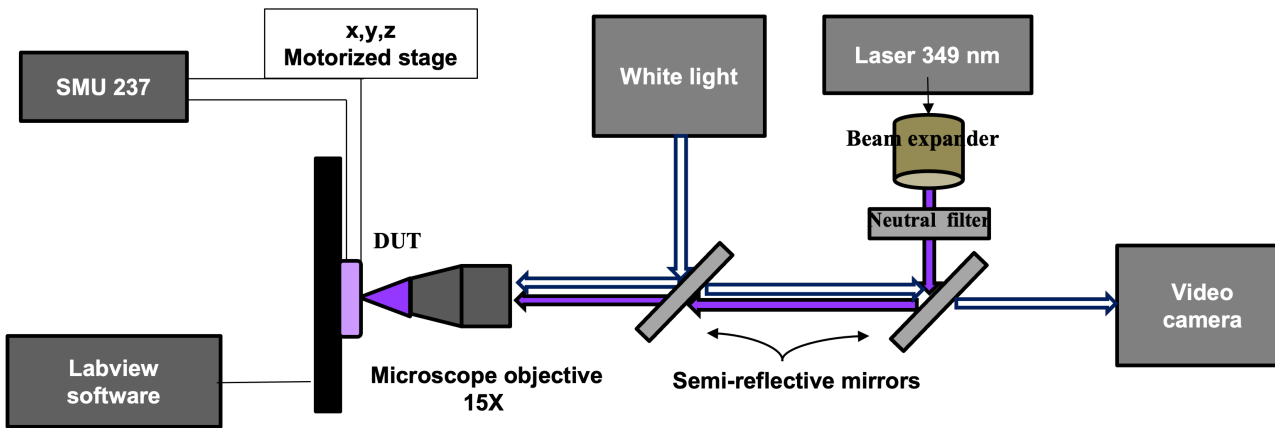


Fig. 1. Schematic representation of the micro-OBIC testbench.

The cross section of the DUT and its periphery is sketched on the Figure 2. The epilayer is $14.8 \mu\text{m}$ thick, n-type doped ($6 \times 10^{15} \text{ cm}^{-3}$). The main junction is realized by ion implantation, at the same time as the field rings, which were carefully designed by Caly Technologies. The diode is then protected by a passivation layer on the front side.

The measurements were realized on two different square-shaped bipolar diodes protected by field rings, namely device 1 and device 2, with and without passivation layer respectively.

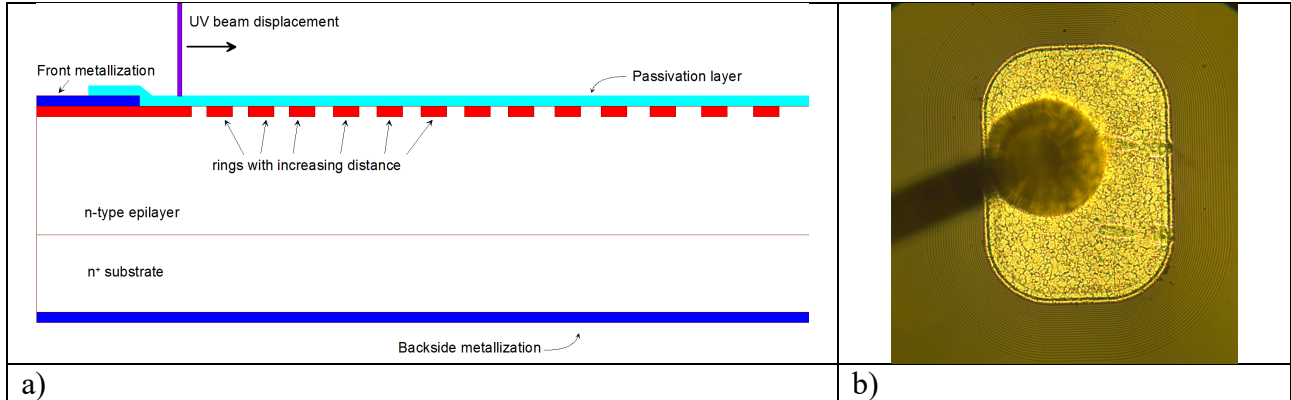


Fig. 2. a) Schematic cross section view of half vertical PiN diodes protected by 22 field rings, b) photograph of the diode with the $50 \mu\text{m}$ (diameter) gold ball bonding

The metallized anode contact is square-shaped, with a side length of $200 \mu\text{m} \times 300 \mu\text{m}$, and a corner curvature radius of $200 \mu\text{m}$ as shown in Fig. 2-b.

This non-destructive technique allows to measure OBIC currents by scanning the outer edge of the biased diode, in order to assess the periphery protection efficiency. OBIC current increases as the electric field intensity increases in the structure. There is no OBIC current on the metallization, neither far from the periphery of the diode. These OBIC current profiles would come in handy to the designer to optimize the breakdown voltage. The diode is protected by 22 field rings as shown in Fig. 2, with increasing spacing between them ($0.07 \mu\text{m}$ from one ring to the next). The distance between the main junction and the first ring is $1.2 \mu\text{m}$. All the rings have the same width ($1.5 \mu\text{m}$).

Inside a vacuum probing chamber, on-wafer measurements of the device demonstrated a stable blocking voltage up to 2 kV as shown in Fig. 3.

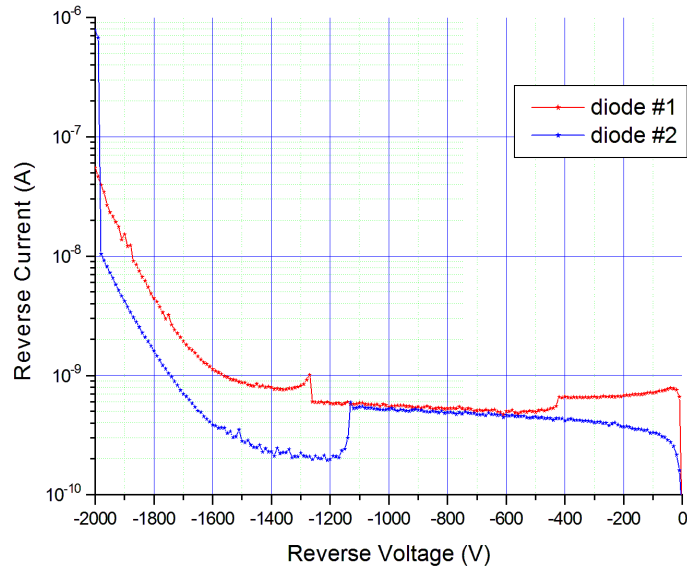


Fig. 3 Reverse characteristics of both devices (diode #1 with polyimide passivation, diode #2 without any passivation)

Results and Analysis

By applying different reverse voltages (up to 500V) to the same diode and re-scanning the very same location, several OBIC currents can be compared to each other, as shown in Fig. 4. As the reverse voltage increases, the OBIC current increases for the same location, due to the increase of the electric field. One can also observe the extension of the space charge region as the reverse voltage increases and the role of outer field rings, witness of the peripheral protection good design.

As the reverse voltage increase, the number of OBIC peaks increase too. From 20 μm up to 97 μm , each maximum is related to the presence of a ring as described in [1] and, more precisely, is located on the outer edge of each ring junction. As the reverse voltage increases, the presence of the rings is more clearly revealed by μ -OBIC. Indeed, the number visible rings by OBIC increase with the reverse voltage. These measurements up to 500V, show the presence of very close rings (between 1.2 μm for the first ring and 2.67 μm for the last ring). One can count all the 22 field rings for a reverse voltage of 500V plus one more peak for the border of the main junction. That means that at 500V all the rings are revealed by the OBIC method.

The amplitude of the maximum doesn't increase much from one voltage to another. The distance between the peaks is in total accordance with the layout of the rings as shown in the figure and in Table 1. Table 1 gives the position of each ring based on its left lateral edge that is oriented towards the main junction when viewed from the cross-section depicted in fig.2a. The OBIC signal amplitude is given for each left lateral edge. Comparing the data from Table 1 and the OBIC profile shown in Fig. 4, each dip in the profile perfectly matches with the left lateral edge of each ring. All the data in the present table were extracted from diode #2 biased under 500 V.

Table 1: Distance from the main junction for ring mask layout and respective OBIC signal values.

Ring number	#1	#2	#3	#4	#5	#6	#7	#8	#9	#10	#11
Distance from main junction (μm)	1.2	3.97	6.81	9.72	12.7	15.75	18.87	22.06	25.32	28.65	32.05
OBIC signal	1.19	3.99	6.99	9.79	12.79	16	18.8	22.21	25.38	28.79	32.2

After measuring diode #1, some scratches appear at the surface of the device under test, due to the sweeping of the laser. In fact, this device was passivated with a polyimide layer, allowing a uniform spreading of the electric field as shown in Fig. 4. With respect to the beam penetration, this additional layer acts as a filter, and the OBIC signal is reduced by a factor of 100 approximately. Nonetheless, Figure 4 shows the benefits of polyimide layer at the top in terms of electric field distribution: at 500V the OBIC current is almost constant whereas Figure 5 shows a decrease in OBIC current value. With a voltage of 300V, one can observe all the rings.

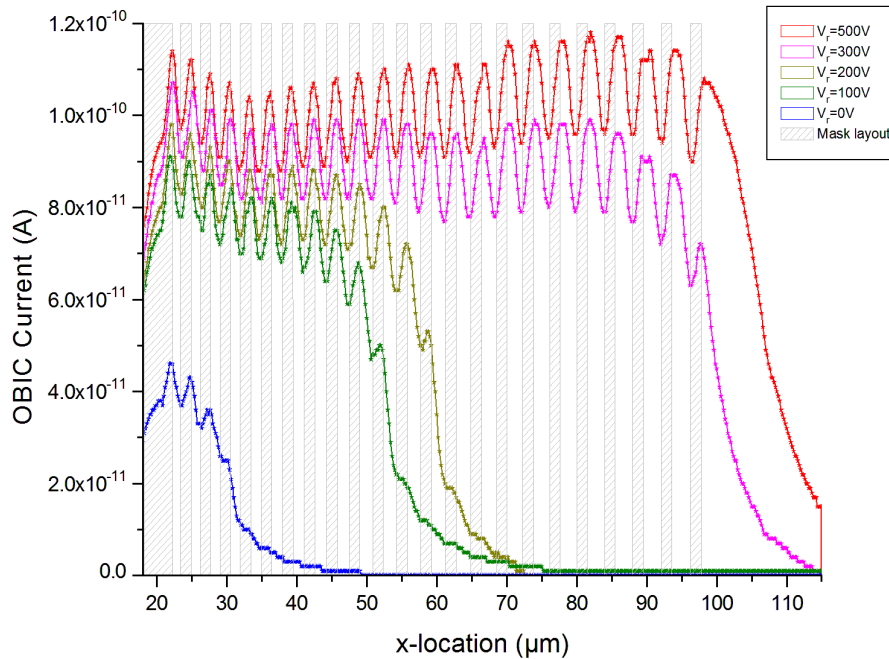


Fig. 4. OBIC currents at the periphery of the diode device #1 (with polyimide) for different reverse voltages (ranging from 0V up to 500V). The mask layout with the spacing between the rings is in grey color.

In order to study the periphery protection without any passivation layer, the polyimide was removed with a very high-density plasma. Then, the same experiment has been performed on diode without polyimide layer at the top. The applied reverse voltage was also limited to 500V. The results are shown in Fig. 5.

Compared to the previous measurements on both devices, performing measurements without the polyimide layer give OBIC profile that reflects the peripheral protection more regular. In both cases, the peaks are related to the distance between the rings, and that is true even for very small distance as low as 1.2 μm.

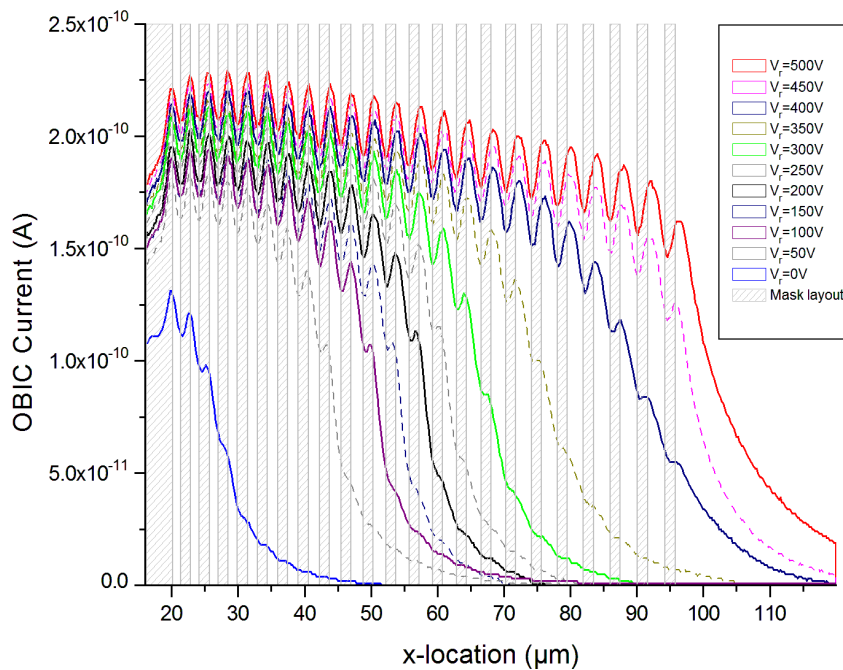


Fig. 5. OBIC currents at the periphery of the diode device #2 (without polyimide) for different reverse voltages (ranging from 0V up to 500V by 50V step). The mask layout with the spacing between the rings is in grey color.

Summary

This paper presents OBIC measurements performed on field rings protected bipolar diodes at different voltages. This test-bench has a well improved spatial resolution compared to the previous OBIC test-bench. We estimated theoretically and experimentally the spatial resolution of the micro-OBIC to be around 1-4 μm . A better resolution is interesting to characterize peripheral protections, such as JTE rings, whose lateral extension is of the order of magnitude of the micron.

JTE rings are directly observable in these experiments, even with narrow distances between each 22 rings. It would be then interesting to complete this study by measurements at higher reverse bias under vacuum and to be closed to the breakdown voltage of the device (1 700 V). It would be also interesting to study these same diodes by other complementary characterization methods such as micro-Raman spectroscopy, SEM/EDX and TOF-SIMS.

References

- [1] P. Godignon et al., this conference (Tu-1A-Inv).
- [2] R. Stengl, High-voltage planar junctions investigated by the OBIC method (1987), IEEE Transactions on electron devices, vol. ED-34, no. 4, pages 911-919.
- [3] C. Sonnevile et al., Materials Science Forum Vol. 1004, (2020) pp. 290-298.
- [4] D. Planson et al., Materials Science in Semiconductor Processing Vol. 94 (2019) pp 116-127
- [5] H. Hamad, C. Raynaud, P. Bevilacqua, S. Scharnholz, D. Planson, Materials Science Forum Vols. 821-823 (2015), p. 223-228.